

UNIVERSITAT POLITÈCNICA
DE CATALUNYA
BARCELONATECH



Fatigue behaviour of Glass-Fiber-Reinforced Polymers: Numerical versus experimental characterization

B. Alcayde*, A. Cornejo*, S. Jiménez*, L. G. Barbu*, M. Merzkirch† and E. Marklund†

PRESENTER NAME: Bàrbara Alcayde

EMAIL: balcayde@cimne.upc.edu

DATE: 05/09/2023

- Introduction
- Constitutive modelling of the GFRP
- Component constitutive model
- Validation and Application Cases
- Conclusions
- Bibliography

Introduction

- Advantages

- High strength
- Low density
- Low maintenance costs
- Good behaviour under fatigue

- Difficulties

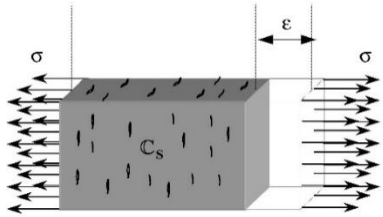
- Multiple failure modes and interaction between them
- Fatigue
- Delamination
- Thermodynamic effects

Application of *composite materials reinforced with long fibers* in the automotive industry (*Fatigue4Light Project*)

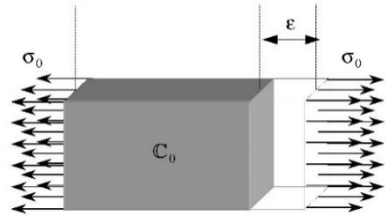


Component constitutive model. Isotropic Damage and Plasticity.

Isotropic damage material



Real damaged solid



Equivalent non-damaged solid

$$\sigma = (1-d)I : \sigma_0 ; \quad \sigma_0 = C : \varepsilon \rightarrow \sigma = (1-d)C : \varepsilon$$

Linear softening

$$d = G[f(\sigma_0)] = \frac{1 - (\tau_{comp}^0 / f(\sigma_0))}{1 + A}$$

A depends on the volumetric fracture energy of the material

Exponential softening

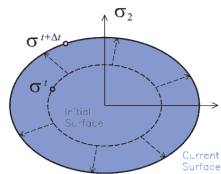
$$d = G[f(\sigma_0)] = 1 - \frac{\tau_{comp}^0}{f(\sigma_0)} \cdot e^{A \left(1 - \frac{\tau_{comp}^0}{f(\sigma_0)}\right)}$$

Plasticity

$$\varepsilon = \varepsilon^e + \varepsilon^p \rightarrow \sigma = C_0 \varepsilon^e = C_0 (\varepsilon - \varepsilon^p)$$

C_0 the isotropic elastic constitutive tensor.

Isotropic Plastic Hardening: Provides an expansion (hardening) or a contraction (softening) of the yield surface.



$$\dot{K} = \dot{\lambda} \cdot H_k = h_k \cdot \dot{\kappa}^p$$

$$\dot{\kappa}^p = \dot{\lambda} \cdot H_k = \dot{\lambda} \cdot \left[h_k : \frac{\partial G}{\partial \sigma} \right] = h_k \cdot \dot{E}^p$$

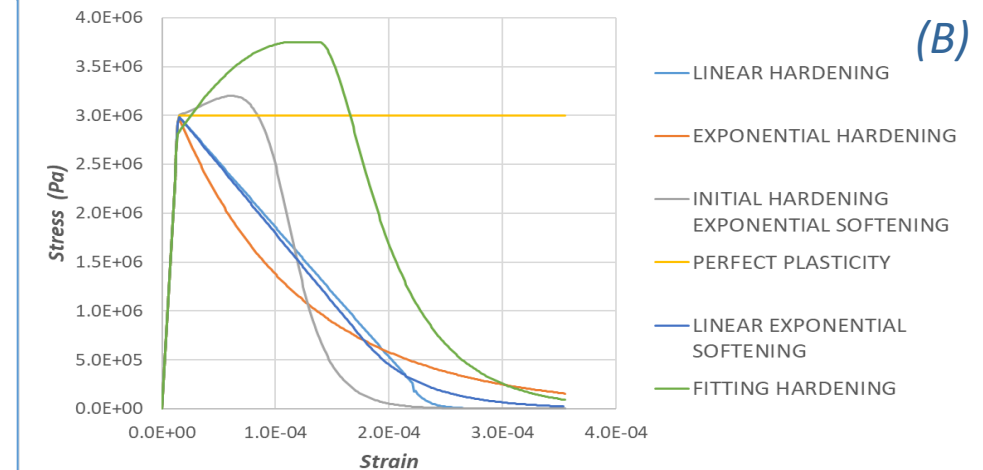
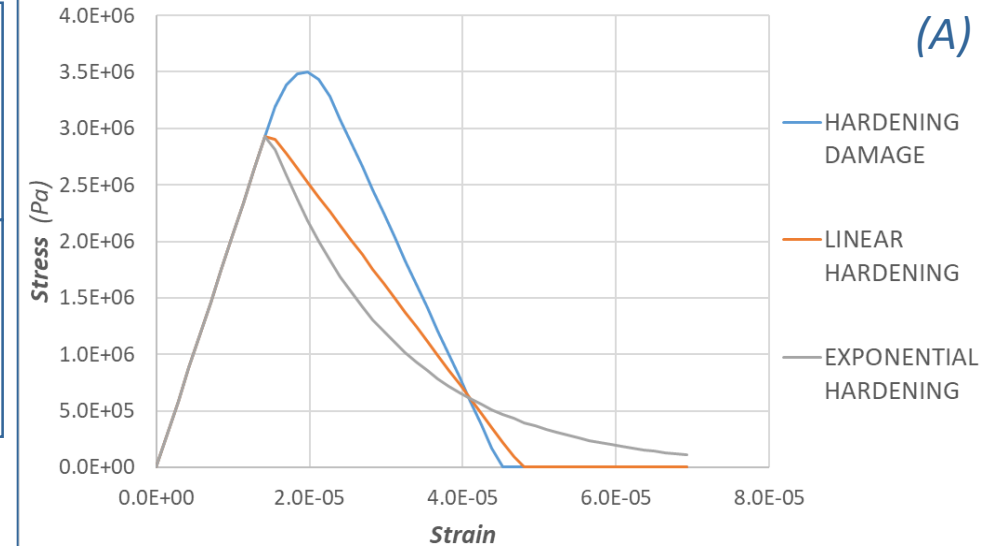
Oliver et al., "Isotropic damage models and smeared crack analysis of concrete" (1990)

Oller, "Nonlinear dynamics of structures" (2014)

Jiménez et al., "On the numerical study of fatigue process in rail heads by means of an isotropic damage based high-cycle fatigue constitutive law" (2022)

Cornejo et al., "Methodology for the analysis of post-tensioned structures using a constitutive serial-parallel rule of mixtures" (2018)

Martinez et al., "Analysis of ultra low cycle fatigue problems with the barcelona plastic damage model and a new isotropic hardening law" (2015)



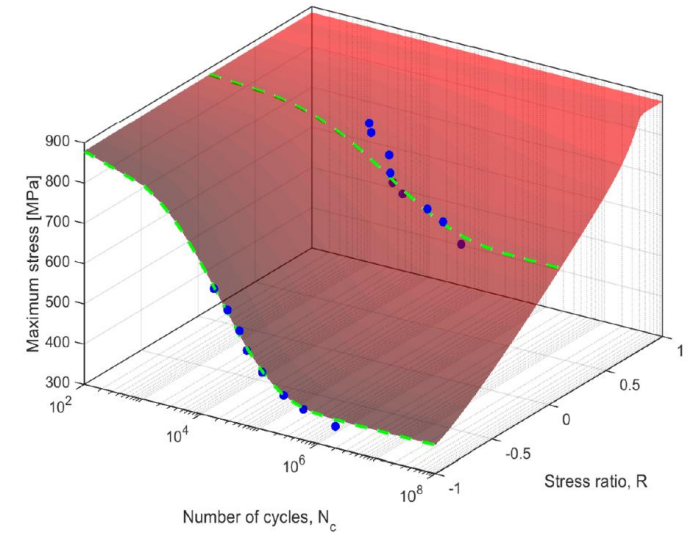
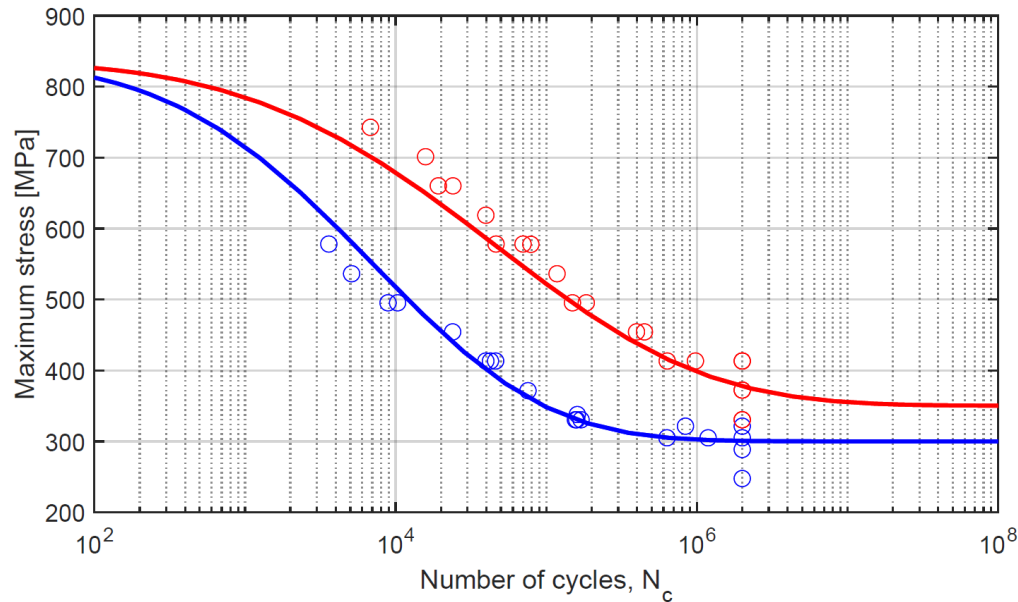
Damage (A) and plasticity (B) developed softening types

Component constitutive model. High Cycle Fatigue (HCF).

Wöhler surface : $S(R, N_c) = S_{th}(R) + (S_u - S_{th}(R))e^{-ALFAT(R) \cdot (\log_{10} N_c)^{BETAF}}$

Reduction factor: $f_{red}(R, N_c, \sigma_{max}) = e^{-B_0 \cdot (\log_{10} N_c)^{BETAF \cdot BETAF}}$

Reversion factor: $R = \frac{\sigma_{min}}{\sigma_{max}}$



$$S_{th}(R) = \begin{cases} S_e + (S_u - S_e) \cdot (0,5 + 0,5 \cdot R)^{STH R1} & \text{for } |R| \leq 1 \\ S_e + (S_u - S_e) \cdot (0,5 + 0,5/R)^{STH R2} & \text{for } |R| > 1 \end{cases}$$

$$ALFAT(R) = \begin{cases} ALFAT + (0,5 + 0,5 \cdot R) \cdot AUX R1 & \text{for } |R| \leq 1 \\ ALFAT - (0,5 + 0,5/R) \cdot AUX R2 & \text{for } |R| > 1 \end{cases}$$

$$B_0 = -\frac{\ln(\sigma_{max}/S_u)}{(\log_{10} N_f)^{BETAF \cdot BETAF}}$$

$$N_f = 10^{\left[-\frac{1}{ALFAT(R)} \cdot \ln\left(\frac{\sigma_{max} - S_{th}(R)}{S_u - S_{th}(R)} \right) \right]^{\frac{1}{BETAF}}} \quad (\text{cycles to failure})$$

$ALFAT, BETAF, STH R1, STH R2, AUX R1$ & $AUX R2$
(model parameters)

Barbu, "Numerical simulation of fatigue processes: application to steel and composite structures" (2016)

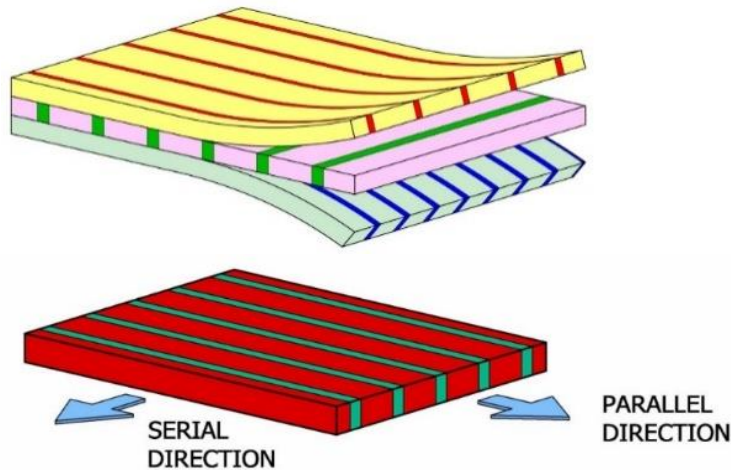
Oller and Oñate, "A continuum mechanics model for mechanical fatigue analysis" (2005)

Jiménez et al., "On the numerical study of fatigue process in rail heads by means of an isotropic damage based high-cycle fatigue constitutive law" (2022)

Constitutive modelling of the GFRP. Serial Parallel Rule of Mixtures Law (SP-RoM).

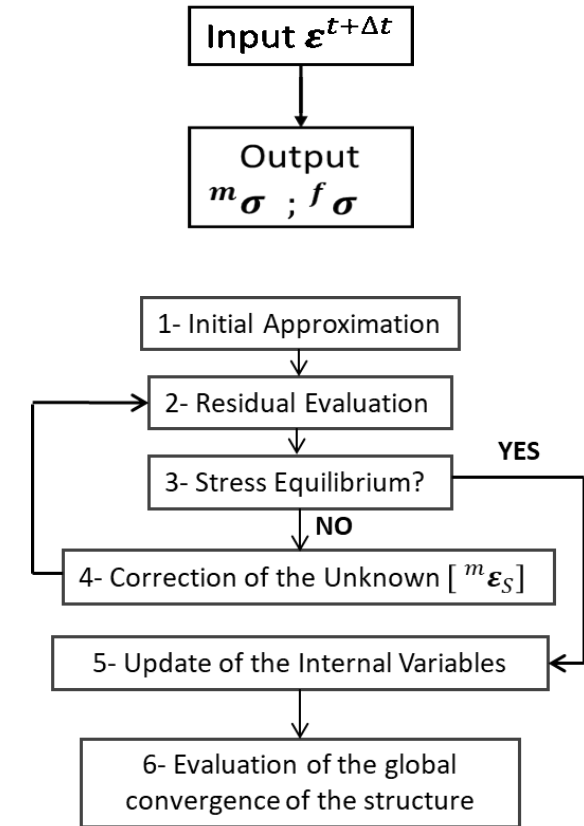
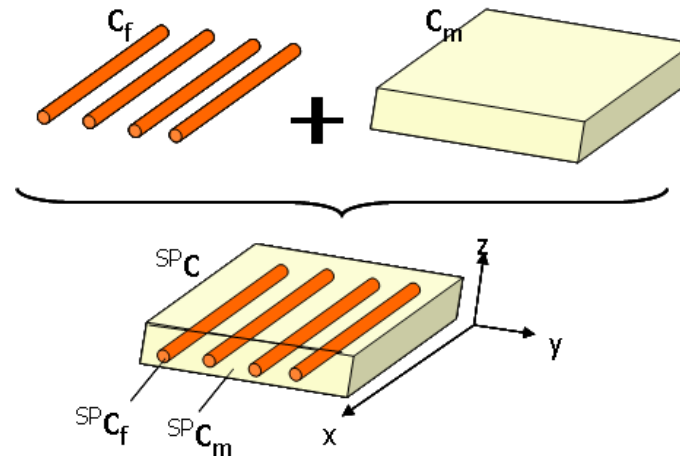
The SP-RoM is a phenomenological homogenization, in which the behaviour of the composite material can be obtained by the constitutive model of its components.

Each interlayer has the same strain
 \Rightarrow the Classical Mixing Theory is applied to each inter-laminar surface



Equilibrium and compatibility equations

Parallel direction	Serial direction
$\begin{cases} c_{\epsilon_P} = {}^f\epsilon_P = {}^m\epsilon_P \\ c_{\sigma_P} = {}^f k {}^f\sigma_P + {}^m k {}^m\sigma_P \end{cases}$	$\begin{cases} c_{\epsilon_S} = {}^f k {}^f\epsilon_S + {}^m k {}^m\epsilon_S \\ c_{\sigma_S} = {}^f\sigma_S = {}^m\sigma_S \end{cases}$



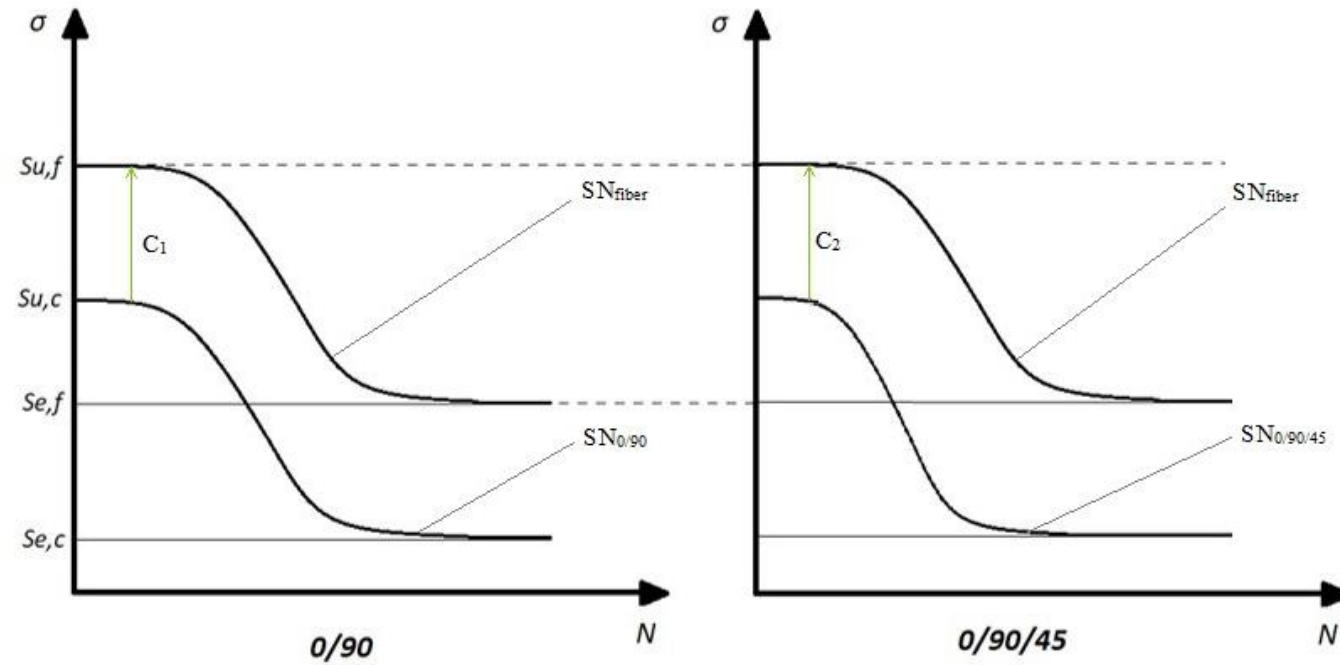
Jiménez et al., "On the numerical study of fatigue process in rail heads by means of an isotropic damage based high-cycle fatigue constitutive law" (2022)
 Rastellini, "Modelización numérica de la no-linealidad constitutiva de laminados compuestos" (2006) Cornejo et al., "Methodology for the analysis of post-tensioned structures using a constitutive serial-parallel rule of mixtures" (2018)
 Martinez et al. "Study of delamination in composites by using the serial/parallel mixing theory and a damage formulation" (2007)

Constitutive modelling of the GFRP. Component characterization.

- **Matrix** suffers *damage-type* degradations.
- **Fiber** suffers from *fatigue* degradation.

SP RoM allows obtaining a factor, C , that relates the stresses in the composite with the ones in longitudinal direction of the fiber.

$$C = \frac{\sigma_f}{\sigma_c}$$



SN curves of different GFRP sequences.

Gerber Parabola:

$$S_a(R = -1) = S_{max}(R = -1) = \frac{\left(\frac{1-R^R}{2} S_{max}(R^R)\right)}{1 - \left(\frac{\left(\frac{1+R^R}{2}\right) S_{max}(R^R)}{S_{ult}}\right)^2}$$

The calibration code requires SN data input for different values of R ($R=0.1$ and $R=-1$)

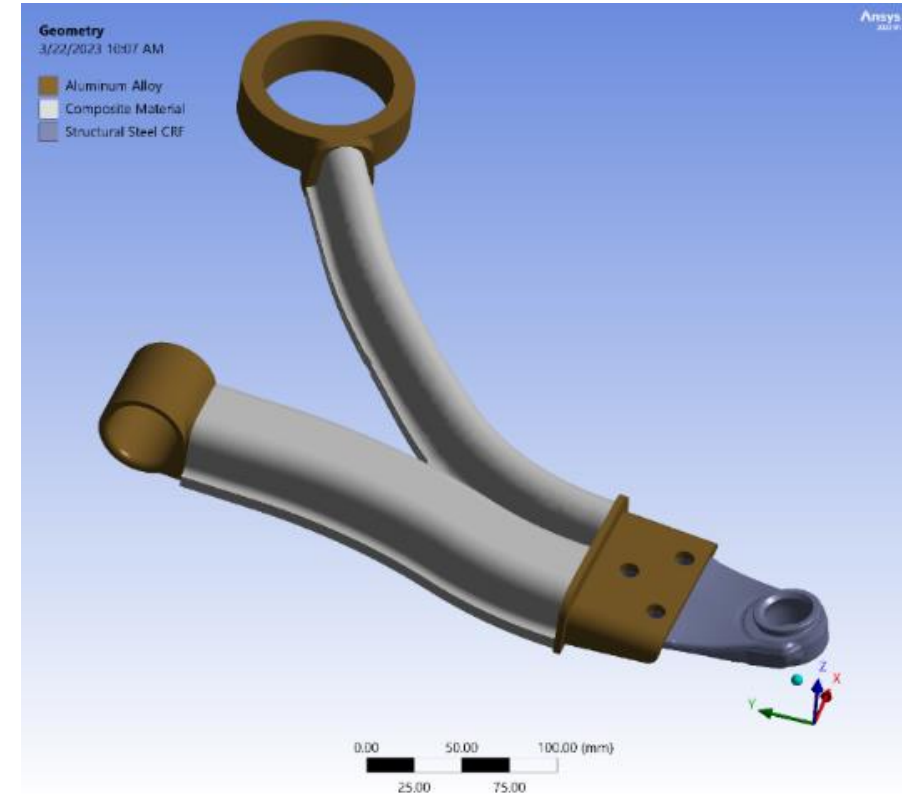
Validation and application cases.

Components
calibration

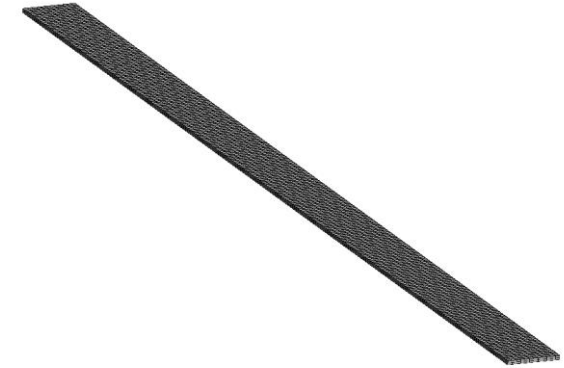
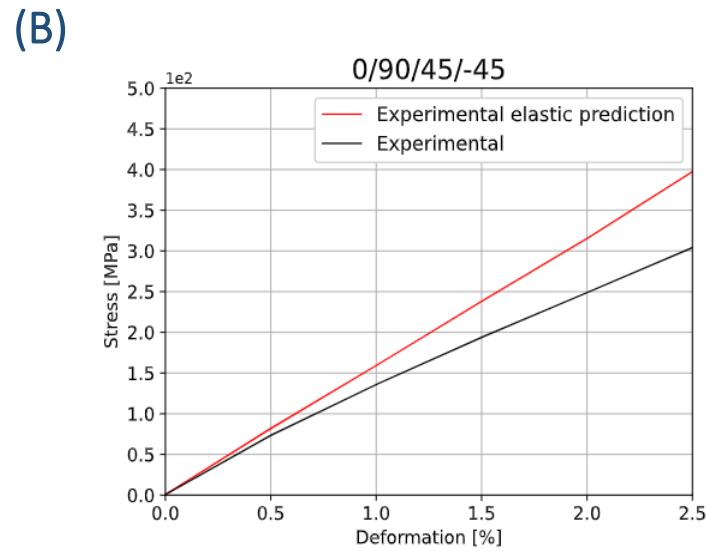
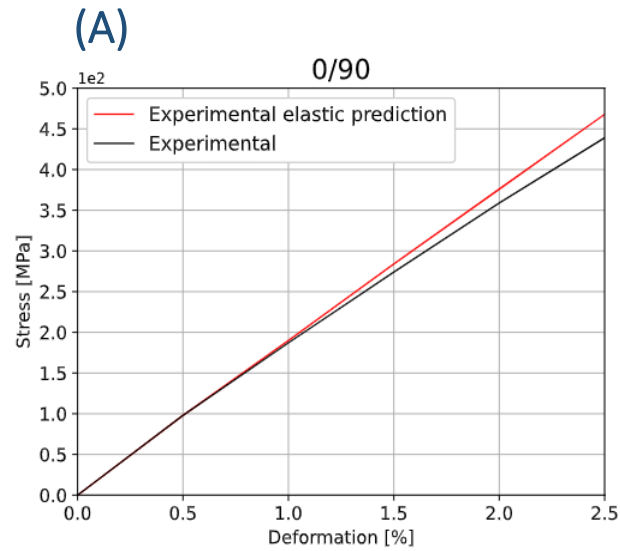
- 0/90
- 0/90/45

LCA sequence

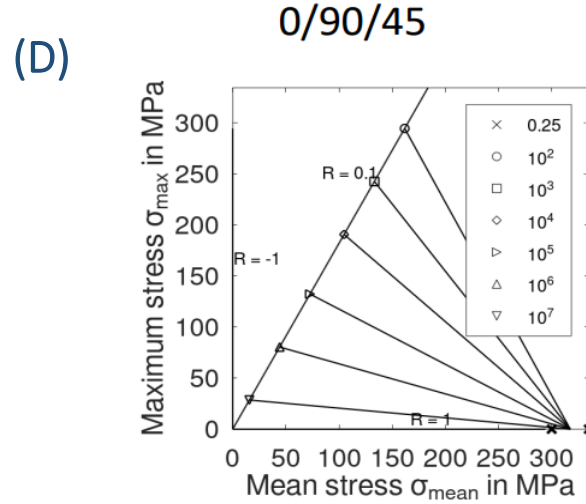
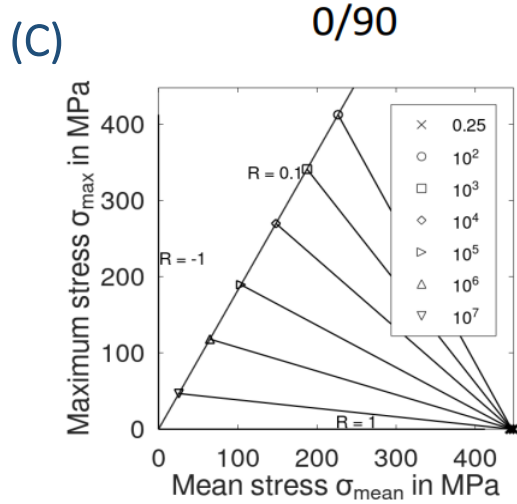
- GFRP
- Hybrid: Aluminium + GFRP
- Application on Low Control Arm (LCA)



Validation and application cases. GFRP components calibration.



Geometry of the specimen.



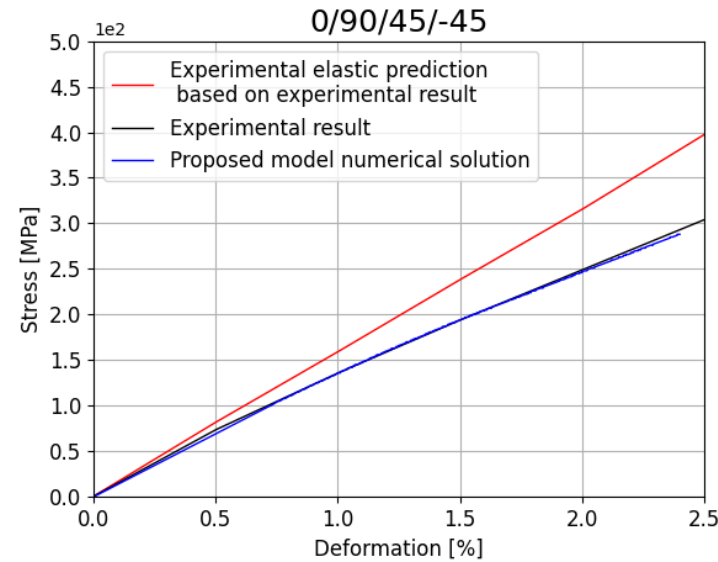
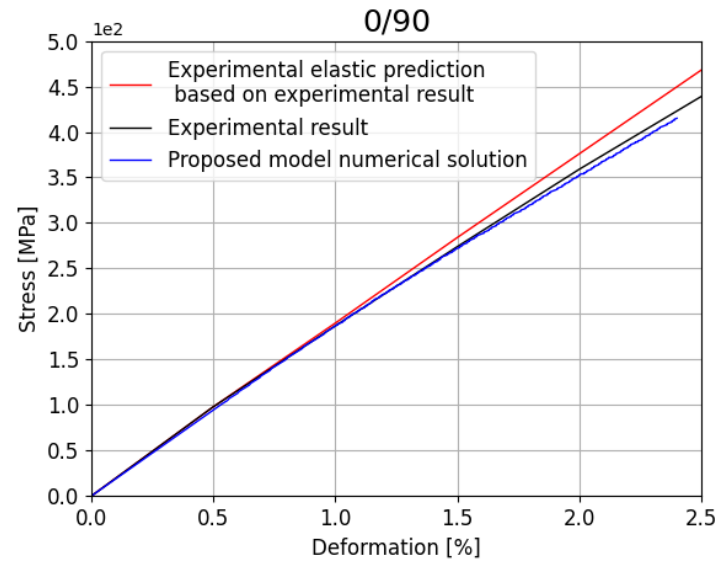
Experimental results of the monotonic (A, B) and the fatigue test (C, D).

0/90/45		0/90	
Nc	Smax	Nc	Smax
1.01	335.15	1.02	449.14
1.01	301.41	1.02	442.61
69.28	296.91	69.16	424.57
174.22	293.91	94.64	407.68
675.32	232.43	1784.56	326.30
2717.35	224.93	1596.50	317.85
13323.52	161.20	33944.39	232.25
18957.73	163.82	21371.82	226.10

Experimental fatigue results.

Validation and application cases. GFRP components calibration.

Experimental results for sequences 0/90 and 0/90/45

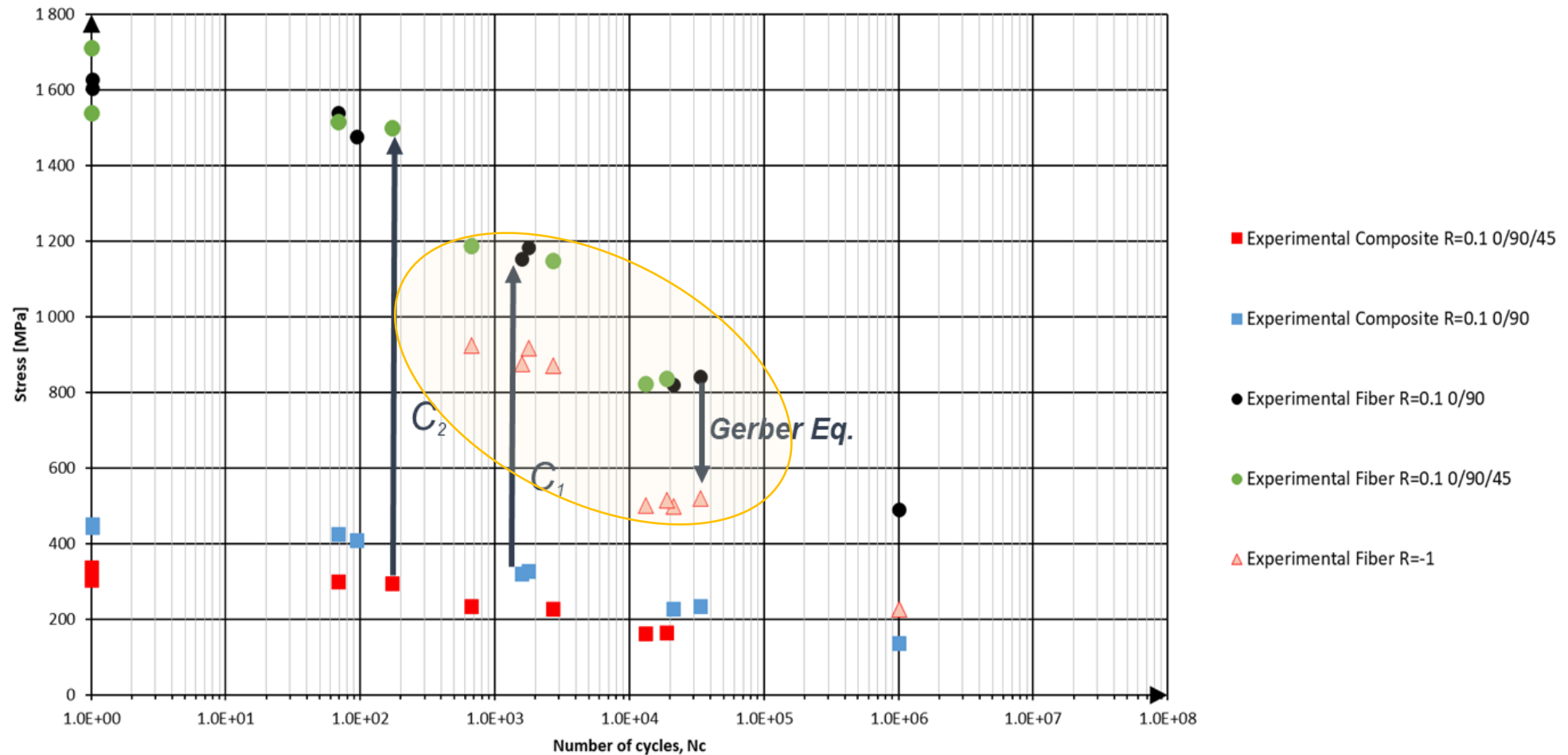


Comparison of the numerical and experimental results of the monotonic test for sequences 0/90 and 0/90/45.

	MATRIX	FIBER
Volumetric Participation (%)	0.55	0.45
Young Modulus (MPa)	$2.58 \cdot 10^6$	$6.88 \cdot 10^7$
Yield stress (MPa)	$3.4 \cdot 10^4$	$1.72 \cdot 10^9$
Poisson	0.35	0.3
Stress Curve Points	[3.4E+07, 3.69E+07, 4.03E+07, 4.36E+07, 4.54E+07, 4.72E+07]	-
Strain Points Curve	[1.34E-02, 1.50E-02, 1.75E-02, 2.00E-02, 2.25E-02, 2.50E-02]	-

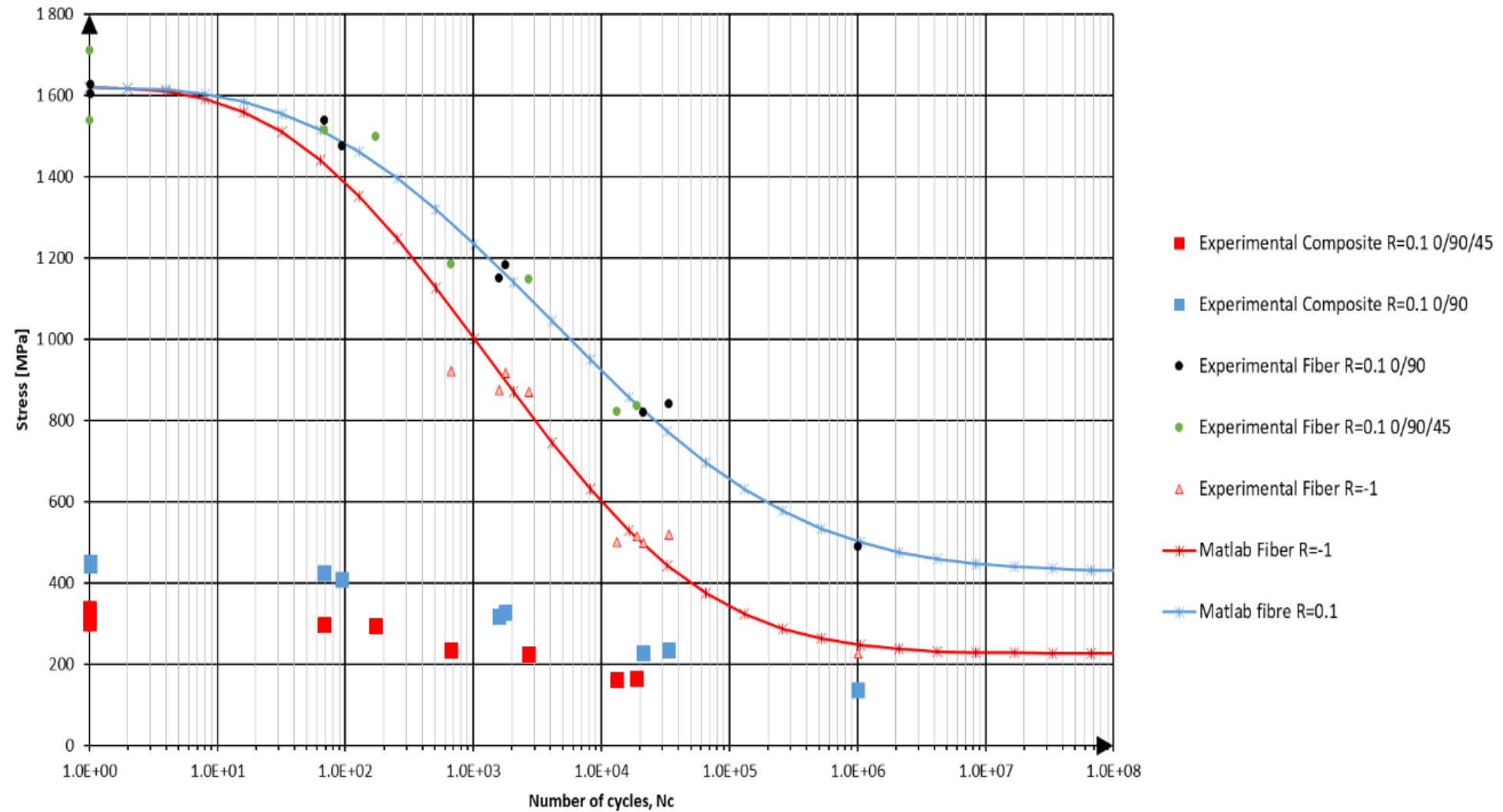
Monotonic fiber and matrix properties for sequences 0/90 and 0/90/45.

Validation and application cases. GFRP components calibration.



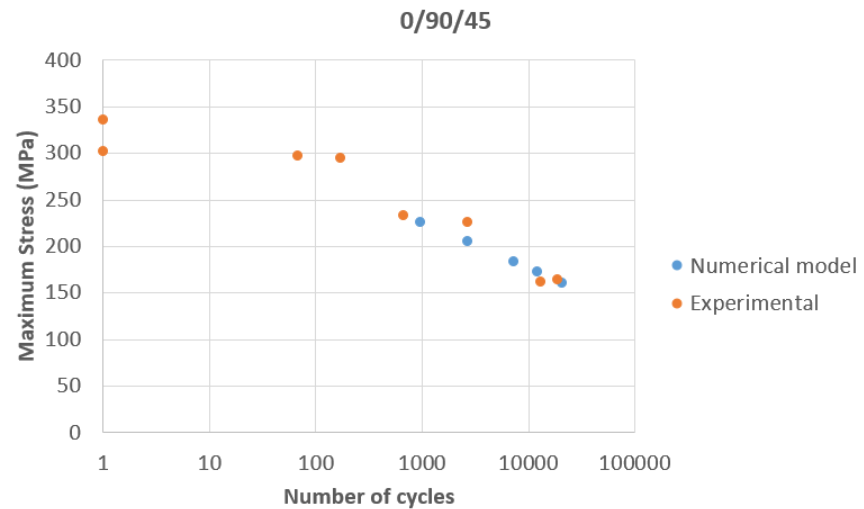
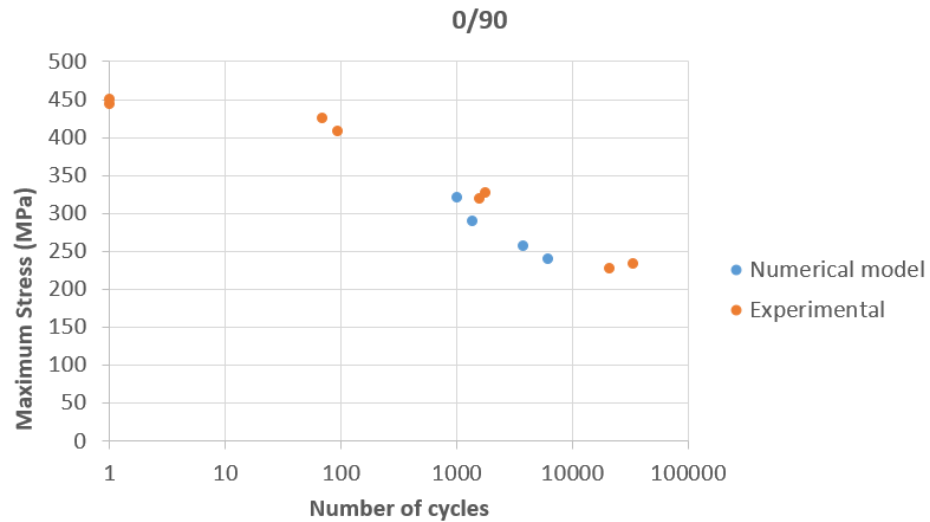
Input data for fatigue fiber fatigue parameters characterization.

Validation and application cases. GFRP components calibration.



Comparison of the SN curve obtained for the fiber from the homogenized experimental data of the composite.

Validation and application cases. GFRP components calibration.



Experimental and numerical data comparison for sequences 0/90 and 0/90/45.

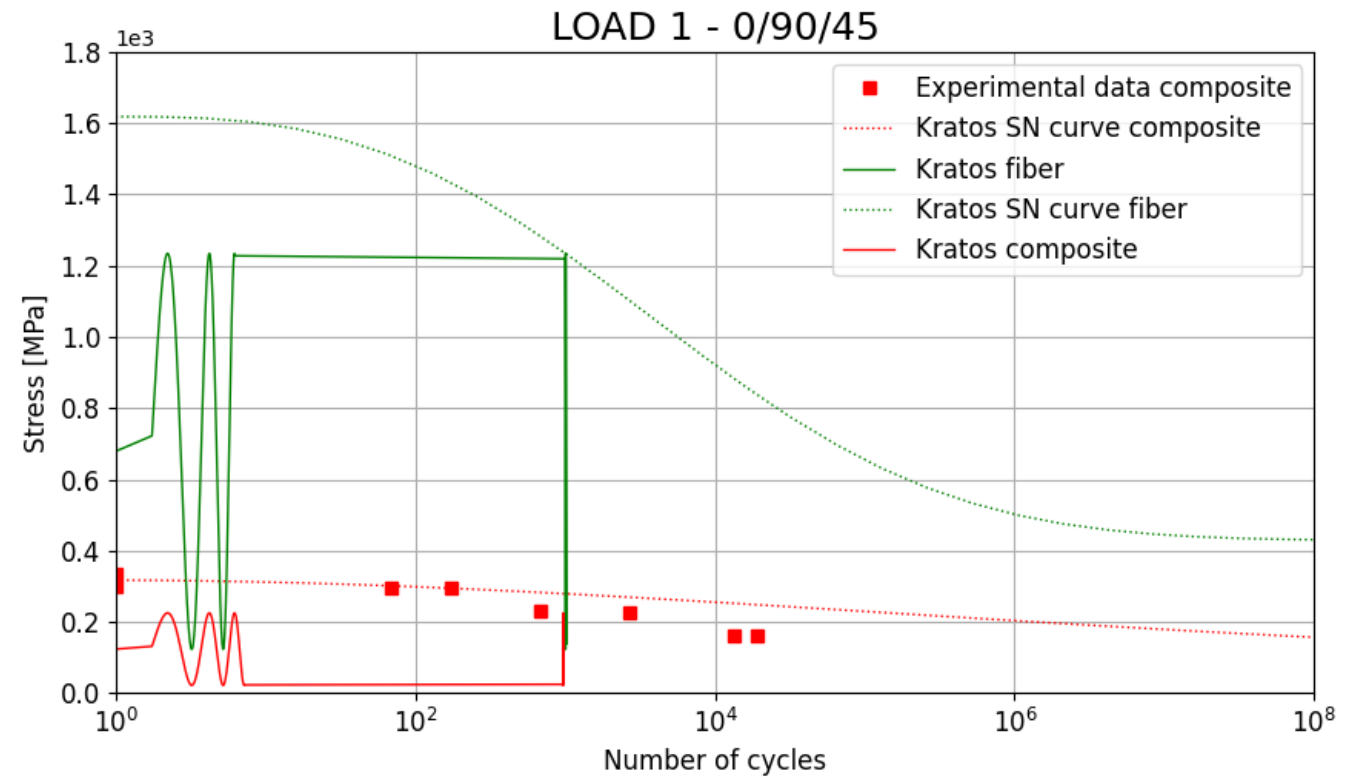
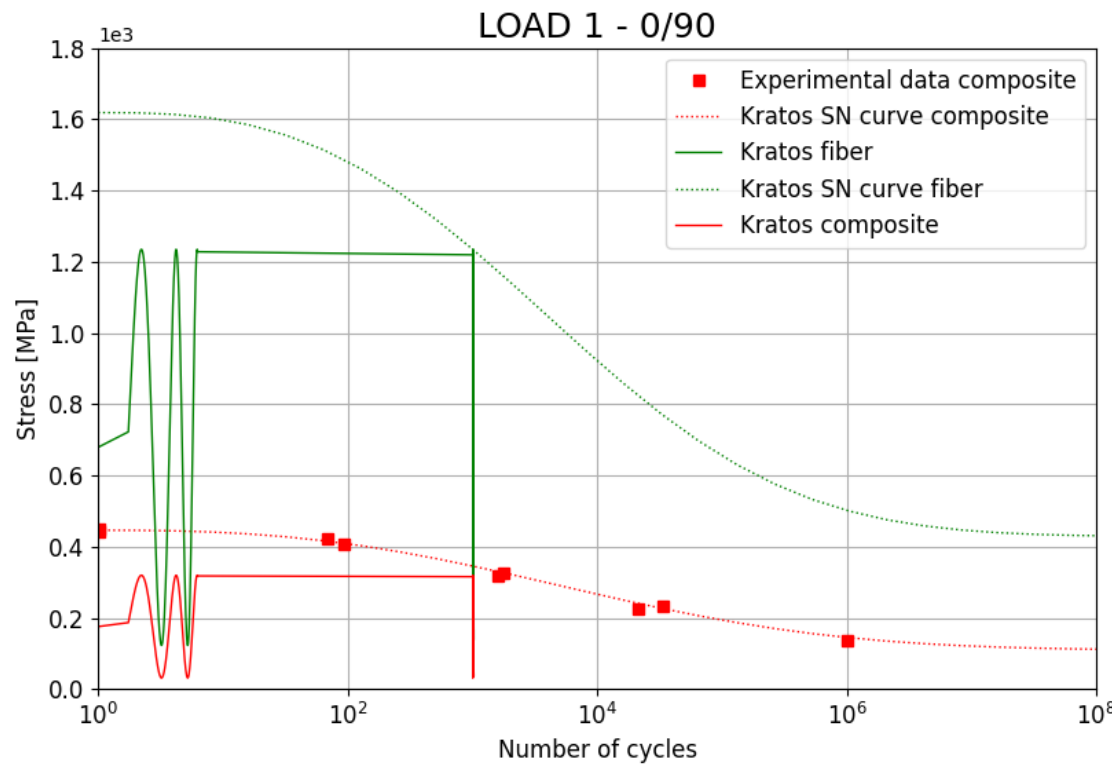
α	STHR1	STHR2	ALFAF	BETAF	AUXR1	AUXR2
0.139	3.224	0.6	0.026	2.843	-0.015	0.002

Fiber fatigue parameters.

LOAD	Max Displ (mm)	0/90		0/90/45/-45	
		Max Stress [MPa]	Number of cycles	Max Stress [MPa]	Number of cycles
1	4.5E-3	320.2	1008	225.65	970
2	4E-3	288.2	1397	204.62	2709
3	3.5E-3	255.8	3770	182.90	7341
4	3.25E-3	238.9	6287	171.48	12250
5	3.0E-3	221.9	21478	159.87	20943

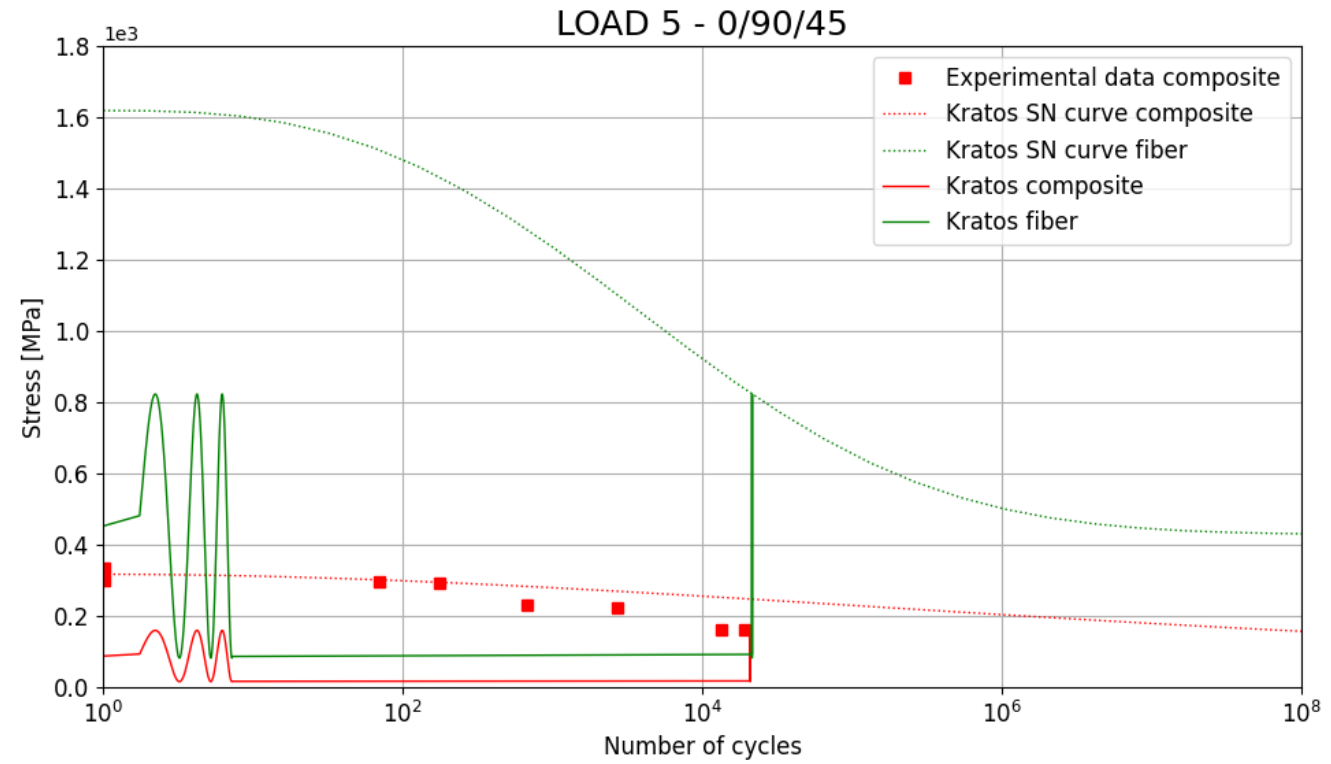
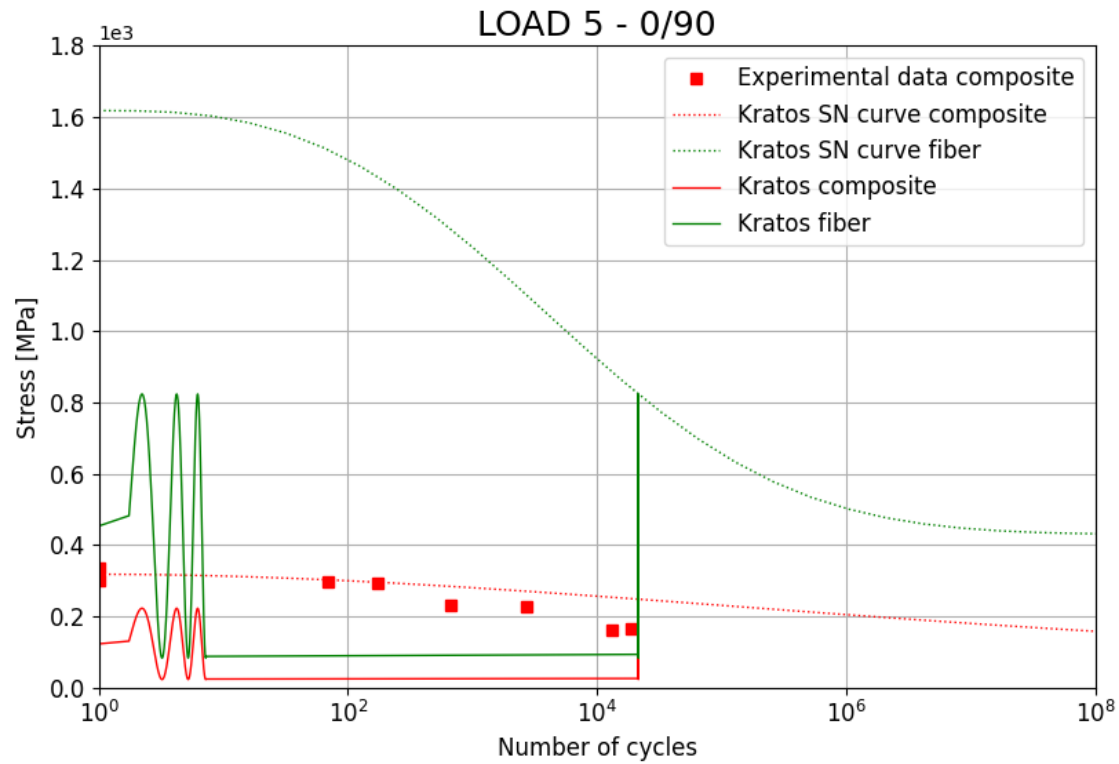
Load scenarios.

Validation and application cases. GFRP components calibration.



Experimental data and SN curves of the composite and fibre for the load scenario 1.

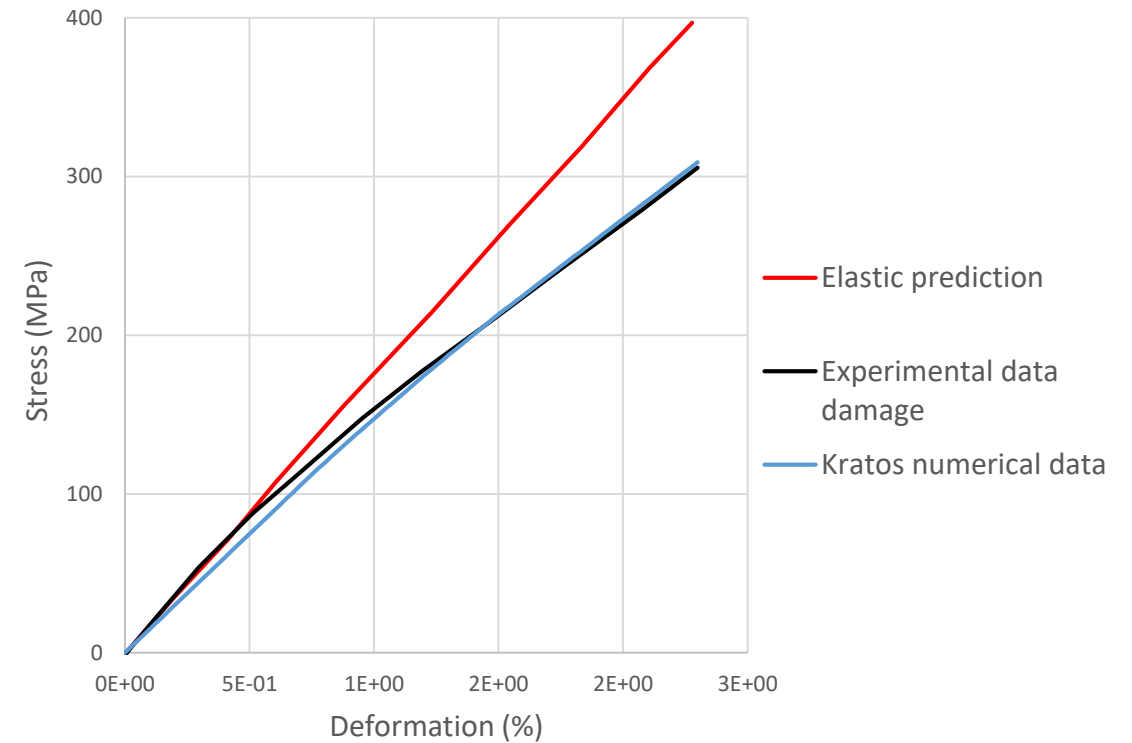
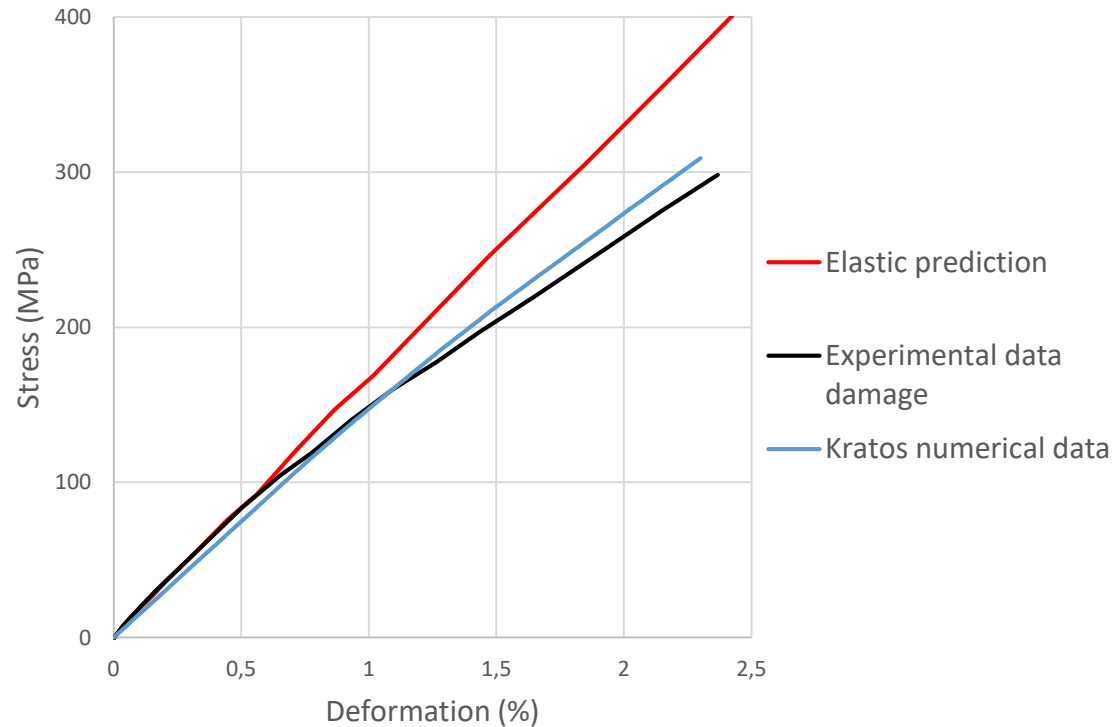
Validation and application cases. GFRP components calibration.



Experimental data and SN curves of the composite and fibre for the load scenario 5.

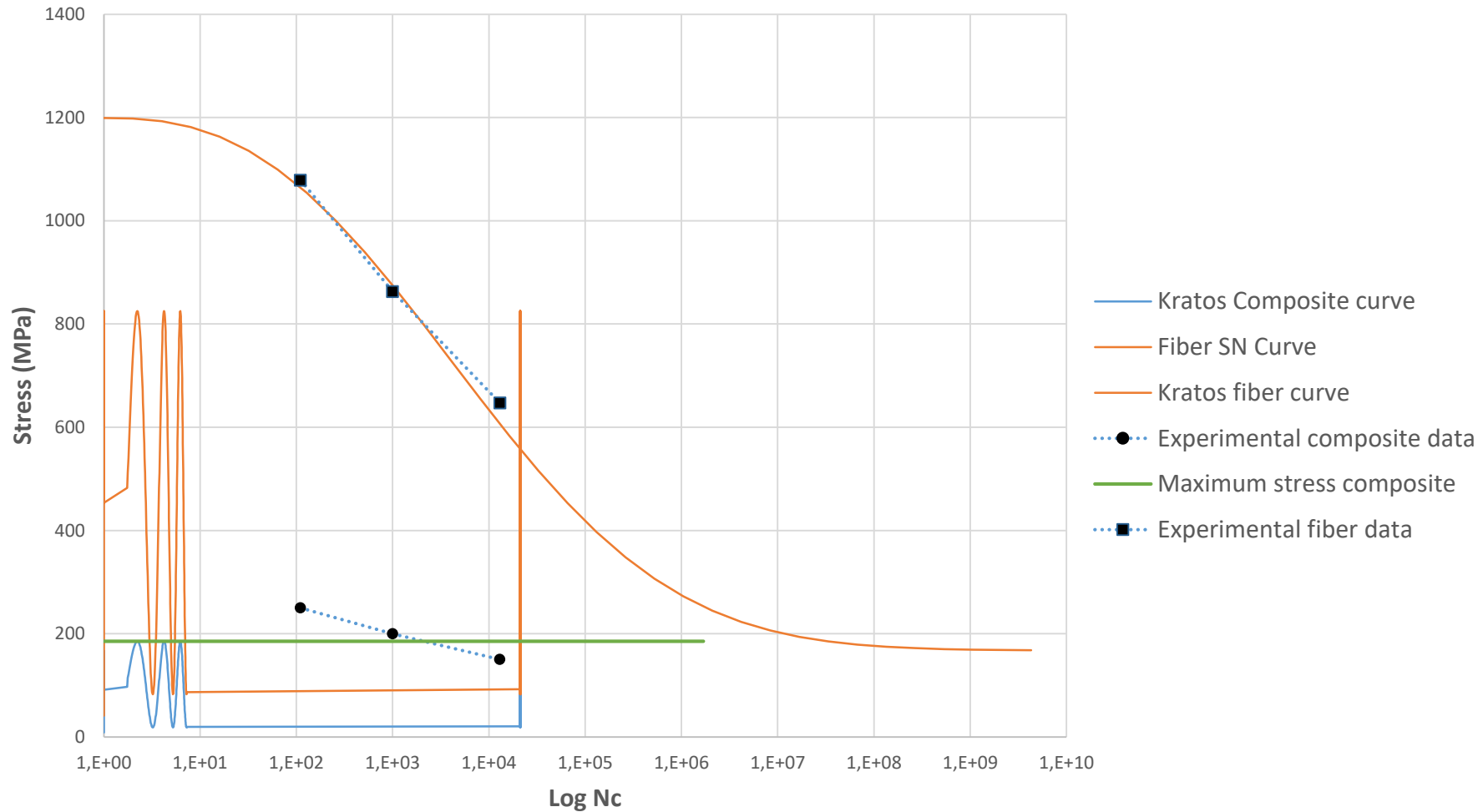
Validation and application cases. LCA – GFRP tension and fatigue.

Selcom EBX400 (biax) NCF / ARALDITE LY 1564, symmetric lay-upc with 6 bi-ax layers (=12 layers)
[(0/90)₂ /±45]_s → [(0/90/0/90/+45/-45/-45/+45/90/0/90/0)]

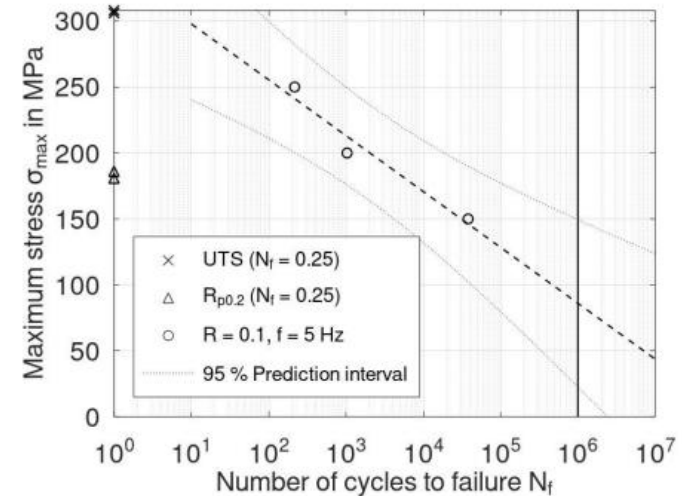
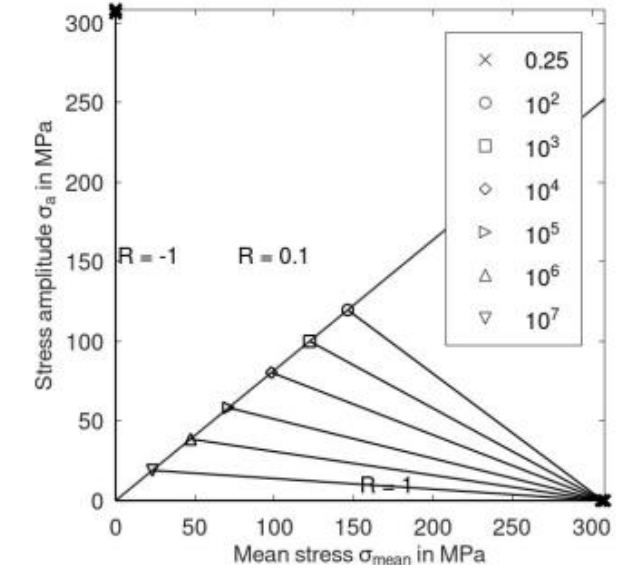


Comparison of the monotonic results obtained for two different specimens with sequence [(0/90)₂/±45]_s.

Validation and application cases. LCA - GFRP tension and fatigue.



Comparison of the fatigue results obtained for the sequence [(0/90)2/±45]s.



Validation and application cases. LCA – Hybrid tension and fatigue.

Al 6082 – T6

Top surface

Biax layer	Tow-layer
90	90
	0
90	90
	0
-45	-45
	45
45	45
	-45
0	0
	90
0	0
	90

Composite/Hybrid midplane

Al 6082 – T6

Bottom surface

Material	Monotonic test	Fatigue test
Fiber	Damage	HCF
Matrix	Damage	Damage
Aluminium	Plasticity	HCF

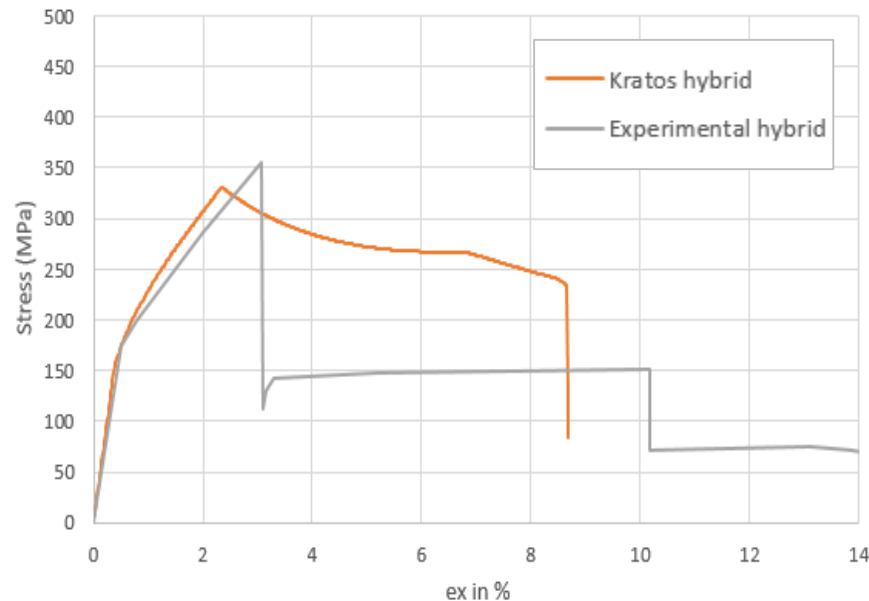
[[90/0/90/0/-45/+45/+45/-45/0/90/0/90]]

$h = 3.47 \text{ mm}$

$h_{Al} = 0.8 \text{ mm}$

$V_{RE,Al} = 45\%$

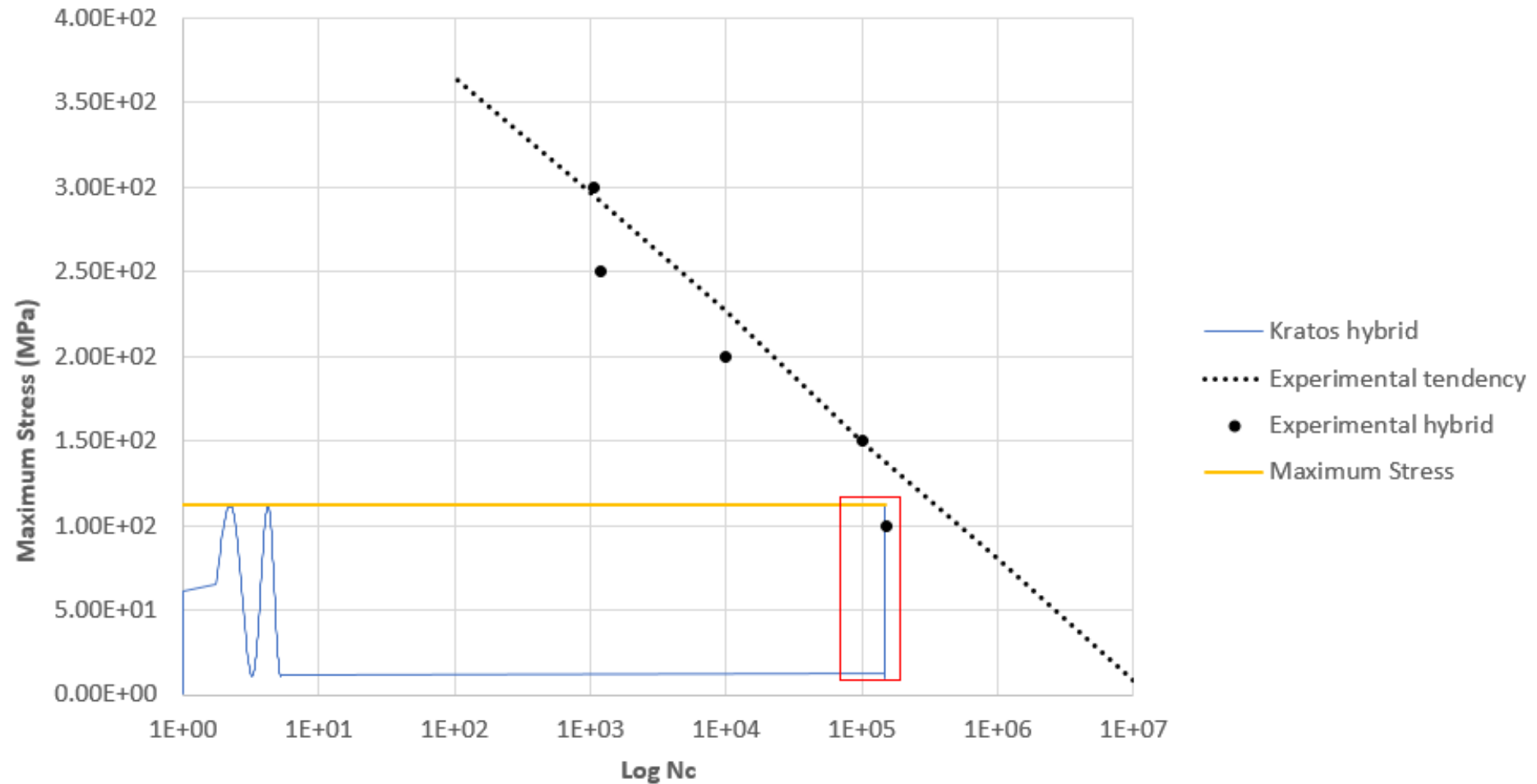
$V_{GFRP} = 55\%$



Comparison of the experimental and numerical data of the hybrid monotonic test.



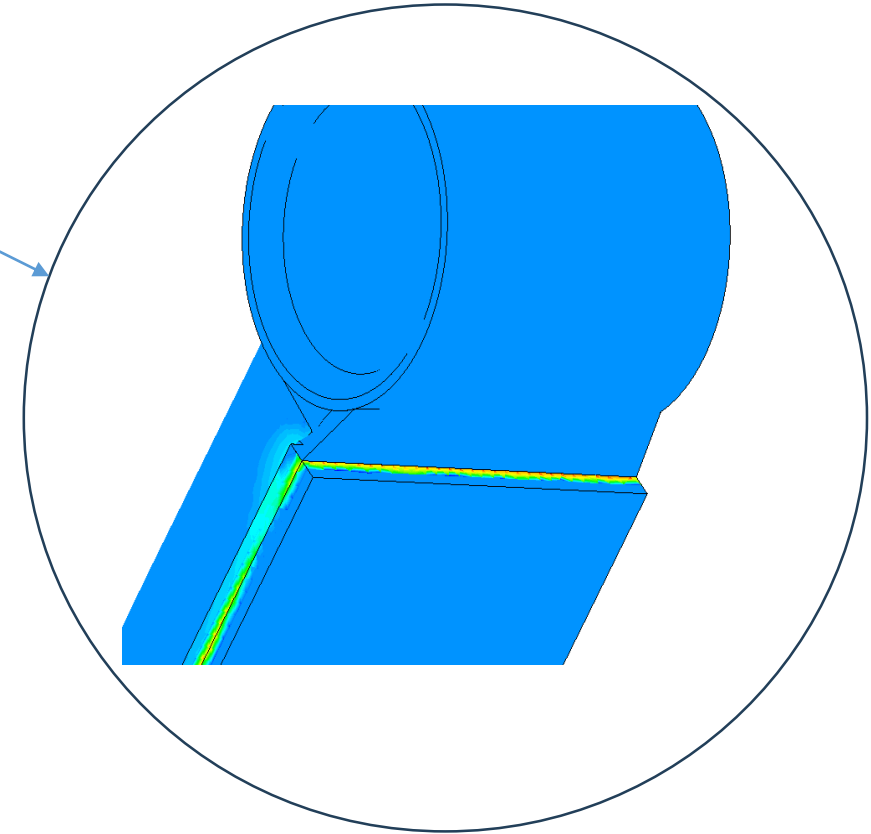
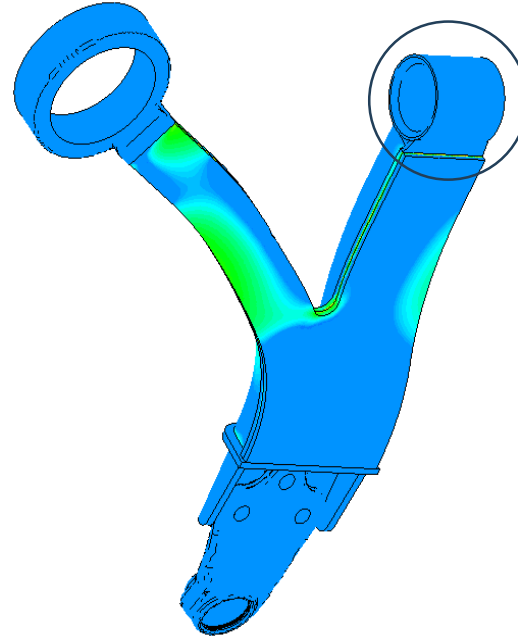
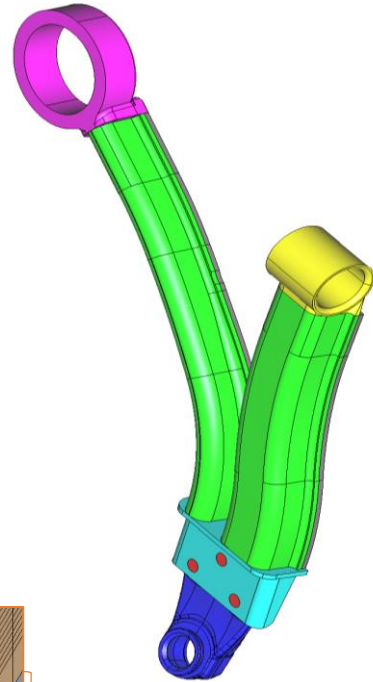
Validation and application cases. LCA – Hybrid tension and fatigue.



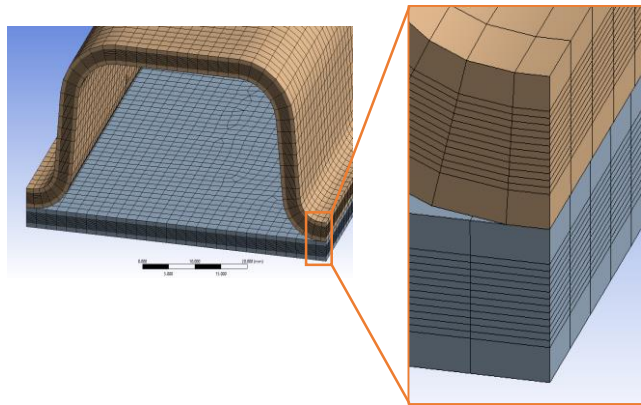
Comparison of the fatigue results obtained for the hybrid.

Validation and application cases. LCA.

Material	Monotonic test
Fiber	Damage
Matrix	Damage
Aluminium	Damage



Damaged areas in the LCA.



Aluminium
Glass/epoxy composite laminate
Aluminium

Element type	Quadratic tetrahedra
Number of elements	317.584
Number of nodes	530.899

Conclusions and future results.

- The correct functioning of the proposed methodology to carry out verified and validated.
- An approach method to predict the properties of the components from the composite data has been proposed and validated.
- The experimental tests for the *hybrid material have been* reproduced numerically.
- Apply the fiber calibrated data in the large scale mesh of the *Low Control Arm (LCA)*.

1. C. Ganesan, P. Joanna, D. Singh, Fatigue life modeling of frp composites: A comprehensive review, *Materials Today: Proceedings* 46 (2021) 555–561. 2nd International Conference on Manufacturing Material Science and Engineering.
2. J. Llobet, A constitutive model for fatigue and residual strength predictions of composite laminates (2019).
3. S. Wicaksono, G. Chai, A review of advances in fatigue and life prediction of fiber-reinforced composites, *Proceedings of the Institution of Mechanical Engineers, Part L: Journal of Materials Design and Applications* 227 (2013) 179–195.
4. G. P. Sendeckyj, *Life Prediction for Resin-Matrix Composite Materials*, 1991.
5. Califano, America & D'Amore, Alberto. (2019). Analysis of a phenomenological model for fatigue of composite materials. *AIP Conference Proceedings*.
6. J. Degrieck and W. Van Paepegem, “Fatigue damage modelling of fibrereinforced composite materials: Review,” *Applied Mechanics Reviews*, vol. 54,no. 4, pp. 279–300, 2001.
7. Passipoularidis, V., & Brøndsted, P. (2010). *Fatigue Evaluation Algorithms: Review*. Danmarks Tekniske Universitet, Risø Nationallaboratoriet for Bæredygtig Energi. Denmark. Forskningscenter Risoe. Risoe-R No. 1740(EN)
8. Teimouri, F., Heidari-Rarani, M., & Aboutalebi, F. H. (2021). An XFEM-VCCT coupled approach for modeling mode I fatigue delamination in composite laminates under high cycle loading. *Engineering Fracture Mechanics*, 249, 107760.
9. Turon, A., Costa, J., Camanho, P. P., & Dávila, C. G. (2007). Simulation of delamination in composites under high-cycle fatigue. *Composites Part A: applied science and manufacturing*, 38(11), 2270-2282.
10. Harper, P. W., & Hallett, S. R. (2010). A fatigue degradation law for cohesive interface elements—development and application to composite materials. *International Journal of Fatigue*, 32(11), 1774-1787.
11. Kiefer, K. (2014). *Simulation of high-cycle fatigue-driven delamination in composites using a cohesive zone model* (Doctoral dissertation, Imperial College London).
12. L. G. Barbu, *Numerical simulation of fatigue processes: application to steel and composite structures* (2016).
13. O. S. S. Oller, E. Oñate, A continuum mechanics model for mechanical fatigue analysis, *Comp. Mater. Sci.* 32 (2) (2005) 175 – 195.
14. L. G. Barbu, A. Cornejo, X. Martínez, S. Oller and A. H. Barbat, Methodology for the analysis of post-tensioned structures using a constitutive serial-parallel rule of mixtures: Large scale non-linear analysis, *Composite Structures*, 216, 315-330 (2019).
15. L. G. Barbu, S. Oller, X. Martinez, A. H. Barbat, High-cycle fatigue constitutive model and a load-advance strategy for the analysis of unidirectional fiber reinforced composites subjected to longitudinal loads, *Composite Structures* 220 (2019) 622–641.1495

16. X. Martinez, F. Rastellini, S. Oller, F. Flores and E. Oñate. Computationally optimized formulation for the simulation of composite materials and delamination failures, *Composites Part B. Engineering* 42.2, 134-144 (2011).
17. Kratos Multiphysics. <<https://github.com/KratosMultiphysics/Kratos>>.
18. GiD. <<https://www.gidhome.com/>>.
19. J. Lubliner, *Plasticity theory*, Macmillan Publishing (New York, USA, 1990).
20. S. O. X. Martinez, E. Barbero, Study of delamination in composites by using the serial/parallel mixing theory and a damage formulation, In *ECCOMAS Thematic conference on mechanical response of composites*, Porto, Portugal (September 12-14, 2007).
21. S. O. X. Martinez, E. Barbero, Mechanical response of composites. chapter: Study of delamination in composites by using the serial/parallel mixing theory and a damage formulation, *ECCOMAS series Edition*, Springer (2008).
22. Javier Oliver, Miguel Cervera, Sergio Oller, and Jacob Lubliner. Isotropic damage models and smeared crack analysis of concrete. 2:945–58, 1990.
23. S. Oller. *Nonlinear dynamics of structures*. Springer, Barcelona, Spain, 2014
24. S. Jiménez, L.G. Barbu, S. Oller, and A. Cornejo. On the numerical study of fatigue process in rail heads by means of an isotropic damage based high-cycle fatigue constitutive law. . *Engineering Failure Analysis*, 131:105915, 2022. ISSN 1350-6307.
25. Alejandro Cornejo, Eugenio Oñate, and Francisco Zarate. A fully Lagrangian formulation for fluid-structure interaction between free-surface flows and multi-fracturing solids. PhD thesis, 12 2020.
26. A. Cornejo, L.G. Barbu, C. Escudero, X. Martínez, S. Oller, and A.H. Barbat. Methodology for the analysis of post-tensioned structures using a constitutive serial-parallel rule of mixtures. *Composite Structures*, 200: 480–497, 2018. ISSN 0263-8223.
27. F. Rastellini. Modelización numérica de la no-linealidad constitutiva de laminados compuestos. PhD thesis, Departament de Resistència de Materials i Estructures a l'Enginyeria (RMEE) - UPC, 2006. Directors: Sergio Oller and Eugenio Oñate.
28. X. Martinez, S. Oller, L.G. Barbu, A.H. Barbat, and A.M.P. de Jesus. Analysis of ultra low cycle fatigue problems with the barcelona plastic damage model and a new isotropic hardening law. *International Journal of Fatigue*, 73:132–142, 2015. ISSN 0142-112.

Acknowledgements

- *This work has been done within the framework of the project Fatigue4Light: Fatigue modelling and fast testing methodologies to optimize part design and to boost lightweight materials deployment in chassis parts.*
- *This project has received funding from the European Union's Horizon 2020 research and innovation programme under grant agreement No 101006844.*